Journal of Physical Organic Chemistry

WILEY

Journal of Physical Organic Chemistry

RESEARCH ARTICLE

Intramolecular Nonbonding Interactions and Geared Phenyl Twisting in Para-Disubstituted 1,4-Diphenylazines: Electron Correlation Effects on Molecular Conformations and Enantiomerization

Kaidi Yang[1] | Harmeet Bhoday[2,3] | Rainer Glaser[3,4]

[1]Department of Chemistry, University of Missouri, Columbia, Missouri, USA | [2]Department of Chemistry, Cornell College, Mount Vernon, Iowa, USA | [3]Department of Chemistry, Missouri University of Science and Technology, Rolla, Missouri, USA | [4]Department of Material Science and Engineering, Missouri University of Science and Technology, Rolla, Missouri, USA

Correspondence: Rainer Glaser (glaserr@umsystem.edu)

Received: 5 September 2025 | **Revised:** 7 January 2026 | **Accepted:** 13 January 2026

Keywords: 1,4-diphenylazines | conformation | electron correlation | enantiomerization | nonbonded through-space interactions

ABSTRACT

The results are reported of potential energy surface (PES) analyses of six symmetrical azines $Y_p-Ph-RC{=}N-N{=}CR-Ph-Y_p$, namely, the benzaldehyde azines **1H**, **2H**, and **8H** with R = H and the acetophenone azines **1M**, **2M**, and **8M** with R = Me. The Y substituents Cl (**1**), Br (**2**), and Me (**8**) were studied because sets of polymorphs **I** (C_2-symmetry, azine twist $\tau \approx 135 \pm 10°$, disrotatory phenyl twists $\phi_i \neq 0°$) and **II** (C_i-symmetry, $\tau = 180°$, conrotatory $\phi_i \neq 0°$) were crystallized for these three azines. The azine-Me groups in (*E*,*E*)-acetophenone azines cause steric strain with the N lone pairs, and this strain is reduced by small rotations about the Az-CH_3 bonds and geared phenyl twisting may lead to C_2- or C_i-structures. The in-depth exploration of the (τ, ϕ_1, ϕ_2) conformational space on the MP2(full)/6-311G* PES of **1M** shows that the enantiomerization of C_2-**1M** to C_2-**1M'** involves, first, one Ph twist inversion to a C_i-like structure, the subsequent inversion of the azine twist in, and the, second, Ph twist inversion on the path to C_2-**1M'**. The essential characteristics of this enantiomerization mechanism apply in general to disubstituted acetophenone azine.

1 | Introduction

Azines are 2,3-diaza derivatives of 1,3-butadienes, and we have been interested in the supramolecular chemistry of azines of the types $X_p-Ph-RC{=}N-N{=}CR-Ph-Y_p$. We studied *unsymmetrical* (R, X, Y)- and *symmetrical* (R, Y, Y)-azines with focus on acetophenone azines (R = CH_3) and benzaldehyde azines (R = H). These materials are "diarenes" in which the two arenes are connected via the azine spacer. It is an intrinsic characteristic of the azine spacer that the two Ph-C bonds cannot be colinear, and there always will be a significant "lateral offset" between the parallel (X = Y) or near-parallel (X ≠ Y) aligned Ph-C bond directions (Scheme 1). The simple feature of the spacer leads to interesting stereochemical consequences. Azine structure depends mainly on the azine twist angle $\tau = \angle$(C=N-N=C) and two phenyl twist angles $\phi_i = \angle$(N=C-C_{ipso}-C_{ortho}).

It is important to understand that the lateral offset provided by the spacer removes any possibility for the two edges of an arenes to be equivalent, and we distinguish inside and outside edges (Scheme 1). An inside edge contains an ortho-carbon C_{oi} that is cisoid with regard to an azine-N ($\phi_i = \angle$(N=C-C_{ipso}-C_{oi}) < 90°, and, vice versa, an outside edge contains an ortho-carbon C_{oo} that is transoid with regard to an azine-N ($\phi_i = \angle$(N=C-C_{ipso}-C_{oo}) > 90°. The description of an edge hydrogen thus requires two subscripts: a first subscript to describe its connectivity to

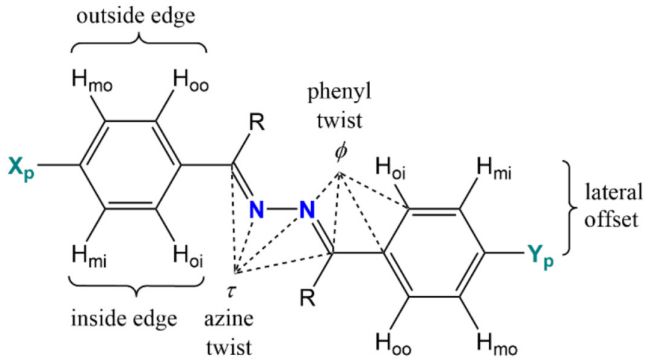

SCHEME 1 | Lateral offset of para-disubstituted azines $X_{para}-Ph-RC{=}N-N{=}CR-Ph-Y_{para}$.

an ortho-C (H_o) or a meta-C (H_m) and a second subscript to distinguish between the inner (H_{oi} and H_{mi}) and outer (H_{oo} and H_{mo}) edges.

Two reviews are available describing the syntheses of azines: their molecular structures and the broad spectrum of their applications [1, 2]. Traditionally, azines are prepared by condensation of carbonyl compounds with hydrazine. Recent advances have greatly improved access to symmetrical and unsymmetrical azines, and these include a nickel-catalyzed synthesis [3] and a route via iminyl radical N – N bond cross-coupling [4]. Perhaps the most important applications of azines are in pharmaceutical chemistry, with azines displaying antimicrobial, antifungal, and anticancer activities [5]. Azines are attracting increased attention for their materials properties. For example, azine-linked covalent organic frameworks serve as electrode materials for energy storage devices [6], and fluorescent azines exhibit promising photophysical and electrochemical properties [7]. Our interest lies with nonlinear optical (NLO) molecular crystalline materials [8–10].

The fabrication of NLO materials rests on the avoidance of centrosymmetry as a minimal requirement and aims at the creation of crystals with high dipole–parallel alignment (HDPA). Our approach aims to create polar layers of parallel aligned diarenes and their polar stacking in the third direction. We developed a nomenclature to distinguish symmetrical and unsymmetrical amphiphiles [11]. Idioteloamphiphiles contain two polar head groups of the same kind (Greek, *idios*) at the ends (Greek, *telos*) of a nonpolar chain. Bolaamphiphiles contain different head groups at the ends of a usually saturated hydrocarbon spacer. Beloamphiphiles are polar and conjugated bolaamphiphiles, and the prefix belo (Greek, *belos*, arrow) reflects their polarity. The key concept guiding the design of these HDPA materials consists in the use of lateral quadrupole–quadrupole interactions of arene–arene contacts to compensate and overcome the electric repulsion associated with dipole–dipole–parallel alignment [11–13]. Indeed, we have been able to fabricate HDPA crystals with several series of donor–acceptor substituted acetophenone azine, the (Me, X, Y)-azines, with polar stacking of beloamphiphile monolayers (BAMs). Initial success came with the methoxy series of acetophenone azines (R = Me) with X = OCH_3 and Y = Cl [14], Br [15], I [16]. This concept also was successfully expanded to several representatives of the phenoxy series (X = OC_6H_5, Y = F, Cl, Br, I) [17, 18], the decyloxy series (X = O$(CH_2)_9CH_3$, Y = F, Cl, Br) [19–22], and the methoxyphenyl series MeO – Ph – Ph – (Me)C=N – N=C (Me) – Ph – Y_{para} (Y = F, Cl, Br, I) [23] of acetophenone azines. The lateral double T-contact is the common supramolecular motif of BAMs to ensure parallel alignment. The achievements of polar order within a beloamphiphile monolayer (PBAM) and of polar stacking of PBAMs depend on the substituents and their interlayer interactions [11, 19]. Hence, we sought to learn about the stereochemistry of symmetrical azines and of the intermolecular interactions in their crystals containing idioteloamphiphile monolayers (IAM) [24, 25], and we reported inventory interaction analyses of 10 symmetrical acetophenone azines **1**–**10** as a function of the Y substituent [26].

Many crystals contain 1,4-diphenylazines with an azine twist and disrotatory phenyl twists so that each azine offers an arene face and an arene edge to all its next neighbors to properly engage in lateral double edge-to-face contacts, the so-called double T-contacts. However, different azine conformations have been observed in crystals. In a prominent example, C_i-symmetric azines without azine twist ($\tau = 180°$) and conrotatory phenyl twists ($\phi_i \neq 0°$) occur in a series of second polymorphs **II** of the isostructural symmetrical acetophenone azines [27] **1M-II** (X = Y = Cl, "**M**" for R = Me) [28], **2M-II** (X = Y = Br) [29], and **8M-II** (**B**, X = Y = Me) [30]. These polymorphs offer a unique opportunity for comparison to the azine-twisted first polymorphs **1M-I** [31] ($\tau = 134.7°$), **2M-I** [32] ($\tau = 131.9°$), and **8M-I** [30] (**A**, $\tau = 142.8°$). Moreover, the crystal structures of the para-substituted (H, Y, Y) benzaldehyde azines **1H** [33] (Y = Cl, "**H**" for R = H) and **2H** [34] (Y = Br) contain entirely planar azines ($\tau = 180°$, $\phi_i = 0°$). In this context, we report here on the results of potential energy surface (PES) analyses of benzaldehyde azines **1H**, **2H**, and **8H** and acetophenone azines **1M**, **2M**, and **8M** to address three important questions. First, we examine theoretical method dependencies by comparison of a proven density functional theoretical (DFT) method and full second-order Møller–Plesset perturbation theory (MP2). Second, we present a detailed theoretical analysis of the effects of the H/CH_3 replacements on the azine carbons on molecular conformation and explain the origin of phenyl twisting in acetophenone azines. Third, results of (τ, ϕ) 2D scans of the PESs inform about the enantiomerization process of helical azines

2 | Computational Section

Conformational preferences of the free acetophenone azines **1M**, **2M**, and **8M** and of their benzaldehyde azine analogs **1H**, **2H**, and **8H** were studied with density functional theory (DFT) [35] at the APFD/6-311G* level; that is, we employed the Austin–Petersson–Frisch functional with dispersion (APFD) [36] together with the 6-311G* basis set [37–39]. In each case, the free azine was completely optimized (C_1) or with various symmetries imposed (C_{2h}, C_i, C_2), and harmonic vibrational frequencies were computed to determine the character of the stationary structure and thermochemical data. All stationary structures were also determined at the MP2(full)/6-311G* level, that is, with the second-order Møller–Plesset perturbation theory [40, 41] including all electrons and using the 6-311G* basis set.

For toluene, we examined conformational preferences at the levels APFD/6-311G*, MP2(full)/6-311G*, MP2(full)/6-311+G(2df,p), and MP2(full)/6-311+G(3df,3pd) and also at higher levels of the Møller–Plesset perturbation theory up to full fourth-order [42] including singles, doubles, triples, and quadruple excitations and with the 6-311G* basis set and the larger 6-311+G(2df,p) and 6-311+G(3df,3pd) basis sets [39], that is, up to MP4(full, SDTQ)/6-311+G(3df,3pd)//MP2(full)/6-311+G(3df,3pd).

Relative energies ΔE and relative free enthalpies ΔG will be reported to compare stabilities of structures **A** and **B** with different symmetries and conformations. The ΔE values are determined via $\Delta E = E_{tot}(\mathbf{A}) - E_{tot}(\mathbf{B})$, and they are most appropriate to characterize the PES. The ΔG values are determined in analogy via $\Delta G = G(\mathbf{A}) - G(\mathbf{B})$ where $G(\mathbf{A})$, for example, is computed with the total energy $E_{tot}(\mathbf{A})$, and the molecular thermal energy TE(**A**) and the molecular entropy $S(\mathbf{A})$ are determined by harmonic vibrational analysis for standard conditions (298.15 K, 1 atm). With $E_{tot}(\mathbf{A})$ reported in Hartree, TE(**A**) in kcal/mol, $S(\mathbf{A})$ in cal/(K·mol), and considering the conversion factor 627.51 kcal/(mol·Hartree), one obtains $G(\mathbf{A})$ in Hartree via $G(\mathbf{A}) = E_{tot}(\mathbf{A}) + TE(\mathbf{A})/627.51 - T{\cdot}S(\mathbf{A})/(1000{\cdot}627.51)$.

The computation of relative enthalpies for **8H** and **8M** following the standard protocol may be associated with some uncertainty because of the very low barriers to rotation around the arene-CH_3 bond. In Section 3.2, we will discuss results of detailed studies of staggered and eclipsed toluene to assess the consequences of the application of the standard process compared to using hindered rotor thermochemistry. In Sections 3.3 and 3.5, we will show that the theoretical level dependency of the toluyl-methyl group's conformational preference is a minor issue because rotations about the Ph-Me bonds are essentially free in **8H** and **8M**. This minor issue must be clearly separated from the more significant theoretical level dependency concerning the phenyl twisting in the acetophenone azines, and we explain in Section 3.8 the underlying electron correlation effect.

While we report free enthalpies, we emphasize throughout the discussion that the conformational spaces of the azines include stationary structures in PES regions with rather low curvatures, and hence, the focus of the present study clearly lies with the PES analyses. In particular, the discussion in Section 3.6 will show that extended essentially flat C_i-type plateau transition regions are relevant to the enantiomerization paths.

Computations were performed with Gaussian 16 [43] on the high-performance computer systems LEWIS (University of Missouri) and MILL (Missouri University of Science and Technology).

3 | Results and Discussion

3.1 | Conformations About the Azine N-N Bond: An Overview

We recently explored the APFD/6-311G* PES of **1M** in regions with significant azine twist to establish the correlation between the azine and phenyl twists [26]. It was found that a given azine twist angle (τ) determined the phenyl twists ϕ_1 and ϕ_2, and we made use of this insight in our current studies of C_2-structures of **2M** and **8M**. Here, we also expanded our study of the conformational space of **1M** in four ways: (a) Additional stationary structures with higher symmetry (C_i and C_{2h}) were located; (b) all stationary structures were located not just at the DFT level but also with an electron correlated method, namely, MP2(full)/6-311G*, that would better account for intramolecular noncovalent interactions (i.e., lone-pair repulsion, CH···N interactions, etc.); (c) the PESs of **2M** and **8M** were characterized as with **1M**; and (d) the corresponding benzaldehyde azines **1H**, **2H**, and **8H** were studied to elucidate steric affects in acetophenone azines.

The relaxed PES scans of the azines as a function of dihedral angle τ provide a first overview of the preferences of the azine conformation (Figure 1) and will discuss details concerning three regions. Region 1 includes the minima of the benzaldehyde azines **1H**, **2H**, and **8H** without azine twist ($\tau = 180°$). Region 2 includes the minima of the acetophenone azines **1M**, **2M**, and **8M** with azine twists $\tau \approx 130°$. Region 3 includes structures of acetophenone azines without azine twist, and this region will be relevant for enantiomerization.

Table 1 lists the total energies and thermochemical data obtained at both levels for standard conditions. Cartesian coordinates of all the optimized structures are provided in the Supporting Information. Relative energies ΔE and ΔG_{298} are listed in Table 2, and frequencies of imaginary modes are collected in Table 3.

3.2 | Conformations About the Ph-Me Bond: Toluene Reference and Nomenclature

The analysis of para-methylacetophenone azine **8M** and para-methylbenzaldehyde azine **8H** (a.k.a. para-tolualdehyde azine) requires vocabulary of the conformation of the methylbenzene moieties, and toluene is the appropriate reference to begin the discussion.

The Me-Ph conformation can be eclipsed (one C-H bond in the plane of the arene, $\mathbf{T_{ec}}$) or staggered (one C-H bond perpendicular to the arene plane, $\mathbf{T_{st}}$). Toluene prefers the staggered structure independent of the theoretical level. Optimization and vibrational analysis of staggered and eclipsed toluene at levels APFD/6-311G*, MP2(full)/6-311G*, MP2(full)/6-311+G(2df,p), and MP2(full)/6-311+G(3df,3pd) showed staggered toluene to be a minimum and eclipsed toluene to be a transition state structure for methyl rotation. We also determined energies at the full fourth-order level of the Møller–Plesset perturbation theory based on three sets of structures, that is, up to MP4(full, SDTQ)/6-311G*//MP2(full)/6-311G*, MP4(full, SDTQ)/6-311+G(2df,p)//MP2(full)/6-311+G(2df,p), and MP4(full, SDTQ)/6-311+G(3df,3pd)//MP2(full)/6-311+G(3df,3pd). Cartesian coordinates of all stationary structures of toluene and relevant energies (Tables S1–S3) are included in the Supporting Information. At the APFD level, the relative energy ΔE is marginal, less than 0.01 kcal/mol, and the relative enthalpy $\Delta G = 1.3$ kcal/mol is essentially due to the higher molecular entropy of staggered toluene. At the MP2 levels, the ΔE value rises to 0.05 kcal/mol, while the relative enthalpy ΔG decreases modestly (Table S3).

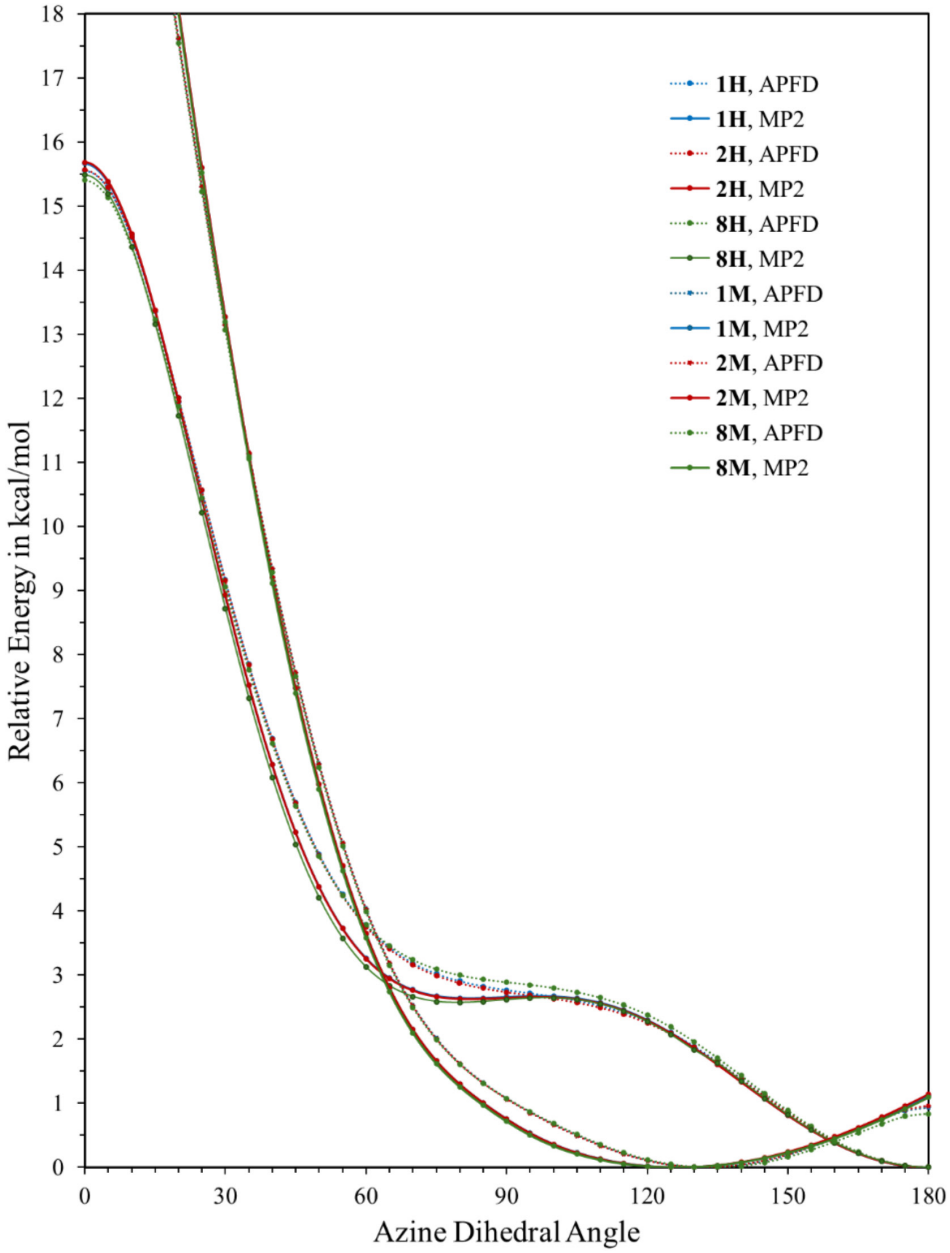

FIGURE 1 | Scans of dihedral angle τ for acetophenone azines **1M**, **2M**, and **8M** and benzaldehyde azines **1H**, **2H**, and **8H** computed at the levels APFD/6-311G* (dashed) and MP2(full)/6-311G* (solid).

The energy difference between $\mathbf{T}_{ec}$ and $\mathbf{T}_{st}$ is minuscule ($\Delta E <$ 0.1 kcal/mol), and the methyl group in toluene rotates freely. The standard protocol for the thermochemical analysis considers the contributions of (3*N*-6) vibrations of "minimum" $\mathbf{T}_{st}$ (including the very soft mode corresponding to the Ph-Me twist) and of (3*N*-5) modes of "transition state structure" $\mathbf{T}_{ec}$, (and the soft Ph-Me mode is the transition mode and not counted). Instead of the standard protocol, the lowest mode ν_1 of "minimum" $\mathbf{T}_{st}$ should be treated as a hindered rotation (HR) [44–46]. Hence, we re-computed the partition functions for $\mathbf{T}_{st}$ in the harmonic approximation but with the replacement of the contribution from the lowest vibrational mode with the appropriate term for the hindered rotation of the CH_3 group [45, 46], and the entries "harm., HR" in Table S1 show the resulting thermodynamic data. With these data, we determined ΔG_{HR} and $\Delta G'_{HR}$ (Table S3), that is, the relative free enthalpies determined with total energies ΔE_{tot} or the ΔE (MP4[SDTQ]) energies, respectively, and thermochemical data TE_{298} and S_{298} corrected for hindered rotation (HR). The ΔG_{HR} and $\Delta G'_{HR}$ values are slightly lower compared to standard ΔG, and in all cases, the conformational preference for staggered toluene is 1 kcal/mol or less.

Eclipsed Me-Ph conformations can be realized in three ways in a symmetrical azine (Scheme 2). The eclipsed C-H bond may have the C→H vector either transoid or cisoid relative to the C→N vector. Azines with both methylbenzene conformations in transoid and cisoid orientations, respectively, are denoted by subscripts "tt" or "cc", respectively, and azine structures with one of both orientations are denoted by subscript "ct" (i.e., cisoid/transoid).

TABLE 1 | Total energies and thermochemical data of azines[a].

Molecule	Total energy E_{tot}	VZPE	Thermal energy TE	Entropy S	Dipole μ	NSS
			APFD/6-311G*			
Benzaldehyde azines						
1H, C_{2h}	−1568.780194	129.52	139.23	131.41	0.00	M
2H, C_{2h}	−5796.464775	128.65	138.70	135.66	0.00	M
Without azine twist						
8H$_{cc}$, C_{2h}	−728.349073	175.89	185.37	125.94	0.00	SOSP
8H$_{ct}$, C_s	−728.349197	175.92	185.96	133.76	0.10	TS
8H$_{tt}$, C_{2h}	−728.349327	176.01	186.56	136.37	0.00	M
Acetophenone azines						
1M, C_2	−1647.367266	164.62	176.24	144.6	1.79	M
1M, C_{2h}	−1647.365771	164.76	175.79	140.53	0.00	TS
2M, C_2	−5875.051935	163.77	175.73	150.21	1.78	M
2M, C_{2h}	−5875.050403	163.91	175.27	144.84	0.00	TS
With azine twist						
8M$_{cc}$, C_2	−806.935082	211.03	222.41	140.64	1.40	SOSP
8M$_{tt}$, C_2	−806.935358	211.12	223.60	152.17	1.26	M
8M$_{ct}$, C_1	−806.935220	211.07	223.00	147.82	1.32	TS
Without azine twist						
8M$_{cc}$, C_{2h}	−806.933727	211.18	221.95	135.26	0.00	TOSP
8M$_{tt}$, C_{2h}	−806.934007	211.25	223.14	147.09	0.00	TS
8M$_{ct}$, C_s	−806.933867	211.22	222.55	142.53	0.10	SOSP
			MP2(full)/6-311G*			
Benzaldehyde azines						
1H, C_{2h}	−1566.831212	127.38	137.63	133.66	0.00	M
2H, C_{2h}	−5793.218128	126.22	136.92	139.95	0.00	M
Without azine twist						
8H$_{cc}$, C_{2h}	−727.009849	174.01	184.10	130.03	0.00	SOSP
8H$_{tt}$, C_{2h}	−727.010063	174.01	184.10	129.99	0.00	SOSP
8H$_{ct}$, C_s	−727.009956	174.01	184.10	131.39	0.07	SOSP
8H$_{apa}$, C_i	−727.010161	174.26	185.35	140.08	0.00	M
8H$_{pa}$, C_1	−727.010161	174.26	185.35	140.08	0.00	M
8H$_{pats}$, C_1	−727.010112	174.14	184.72	135.73	0.04	TS
Acetophenone azines						
1M, C_2	−1645.240746	163.13	175.25	148.09	2.05	M
1M, C_i	−1645.239130	163.13	174.70	142.84	0.00	"TS"
1M, C_{2h}	−1645.238669	162.70	173.87	137.46	0.00	SOSP
2M, C_2	−5871.627744	162.05	174.58	153.88	1.83	M

(Continues)

TABLE 1 | (Continued)

Molecule	Total energy E_{tot}	VZPE	Thermal energy TE	Entropy S	Dipole μ	NSS
2M, C_i	−5871.626101	162.01	174.01	148.97	0.00	"TS"
2M, C_{2h}	−5871.625614	161.47	173.16	144.63	0.00	SOSP
With azine twist						
$\mathbf{8M_{ig}}$, C_2	−805.418814	210.02	222.97	153.58	1.73	M
$\mathbf{8M_{og}}$, C_2	−805.418895	210.06	222.98	152.90	1.67	M
$\mathbf{8M_{mg}}$, C_1	−805.418855	210.04	222.98	154.60	1.70	M
$\mathbf{8M_{mgts}}$, C_1	−805.418782	209.911	222.36	150.34	1.70	TS
Without azine twist						
$\mathbf{8M_{cc}}$, C_{2h}	−805.416432	209.29	220.32	134.18	0.00	FOSP
$\mathbf{8M_{tt}}$, C_{2h}	−805.416663	209.27	220.30	134.17	0.00	FOSP
$\mathbf{8M_{ct}}$, C_s	−805.416547	209.28	220.31	135.57	0.08	FOSP
$\mathbf{8M_{apa}}$, C_i	−805.417265	210.02	223.01	157.68	0.00	"M"
$\mathbf{8M_{pa}}$, C_1	−805.417292	210.03	223.02	158.26	0.00	"M"
$\mathbf{8M_{pats}}$, C_1	−805.417134	209.91	222.40	153.23	0.09	TS
$\mathbf{8M_{apafp}}$, C_i	−805.416761	209.62	221.60	143.92	0.00	SOSP

[a]Total energies E_{tot} in Hartree, vibrational zero-point energies (VZPE) in kcal/mol, thermal energies TE in kcal/mol, entropies S in cal/(mol·K), and dipole moments μ in Debye. Nature of the stationary structures (NSS): minimum (M), transition state (TS), second-order saddle point (SOSP), and fourth-order saddle point (FOSP).

Staggered Me-Ph conformations also can be realized in three ways in a symmetrical azine, and two notations are used to distinguish the resulting structures depending on the absence or presence of an azine twist. In the absence of an azine twist, that is, in C_i-symmetric azine structures, the C→H vectors of the perpendicular C→H bond vectors of both methylbenzenes may be antiparallel aligned, and such a structure is denoted by subscript "apa". An azine without azine twist and its two perpendicular C→H vectors parallel aligned will retain its C_i-type overall shape but must be asymmetric and is denoted by subscripts "pa" (i.e., parallel aligned). Options for a C_2-type twisted azine are illustrated in the bottom row of Scheme 2 with Newman projections down the N-N bond and showing only those C-H bonds that are close to perpendicular to the arene planes. A C_2-type twisted azine has an "inner groove", the space between the two planes containing the arenes enclosing dihedrals of about 130° or less. In C_2-symmetric azine structures, the perpendicular C-H bonds of both methylbenzenes may point into the inner groove or in the opposite direction (i.e., into the "outer groove"), respectively, and the resulting structures are denoted by subscripts "ig" or "og", respectively. A twisted azine structure with one perpendicular C→H bond pointing into the minor groove and the other into the outer groove, such an azine will retain its C_2-type overall shape but must be asymmetric and is denoted by subscripts "mg" (i.e., mixed grooves).

3.3 | Benzaldehyde Azines: Level Dependency of the Methylbenzene Conformation

The 4-halobenzaldehyde azines feature neither azine nor phenyl twists, and the planar structures C_{2h}-**1H** and C_{2h}-**2H** are minima at both theoretical levels. The structures of the 4-tolualdehyde azine **8H** also feature perfectly planar or near-planar Ph-CH=N-N=CH-Ph moieties, while theoretical level dependencies occur for the Ph-Me conformations (Figure 2).

At the APFD/6-311G* level, the Ph-Me conformations are eclipsed with a preference for the in-plane methyl C-H bonds being transoid. C_{2h}-$\mathbf{8H_{tt}}$ is the minimum, C_{2h}-$\mathbf{8H_{cc}}$ is a second-order saddle point (SOSP), and C_s-$\mathbf{8H_{ct}}$ is the transition state structure for methyl rotation in C_{2h}-$\mathbf{8H_{tt}}$ with a rotational barrier A_{rot} of merely $\Delta G = 0.26$ kcal/mol.

At the MP2(full)/6-311G* level, the Ph-Me conformations are staggered and there are two isoenergetic minima C_1-$\mathbf{8H_{pa}}$ and C_i-$\mathbf{8H_{apa}}$. We also located the structure with one staggered and one eclipsed Ph-Me bond and C_1-$\mathbf{8H_{pats}}$ functions as the transition state structure for methyl rotation with barrier A_{rot} of merely $\Delta G = 0.70$ kcal/mol. These structures and the rotational barrier are in line with properties of toluene (vide supra). The three stationary structures C_{2h}-$\mathbf{8H_{cc}}$, C_{2h}-$\mathbf{8H_{tt}}$, and C_s-$\mathbf{8H_{ct}}$ with two eclipsed Ph-Me conformations each all correspond to the SOSPs and feature two imaginary modes associated with Ph-Me bond rotations (Table 3).

3.4 | Para-Haloacetophenone Azines

At the APFD level, the C_{2h}-**1M** structure ($\tau = 180°$, $\phi_1 = \phi_2 = 0°$) was easily located and found to be a transition state structure. The imaginary mode **i**20.1 cm^{-1} corresponds to the expected rotation about the N-N bond and facilitates C_2-**1M** ⇌ C_2-**1M'** enantiomerization with concomitant changes of the azine and the phenyl twists. However, a theoretical method dependency occurs in that the C_{2h}-**1M** structure corresponds to a SOSP at the MP2/6-311G* level. The imaginary modes **i**23.6 cm^{-1} and **i**34.9 cm^{-1} correspond

TABLE 2 | Relative energies computed at APFD/6-311G* and MP2/6-311G* levels[a,b].

	Relation	ΔE	ΔG	Relation	ΔE	ΔG
Azine Conform.	**Me-Ph conf.**			**Azine conf.**		
	Benzaldehyde azines					
	APFD/6-311G*					
No azine twist	**8H$_{cc}$** vs. **8H$_{tt}$**	0.16	2.08			
C_{2h} or C_{2h}-like	**8H$_{ct}$** vs. **8H$_{tt}$**, A_{rot}	0.08	0.26			
	MP2/6-311G*					
No azine twist	**8H$_{cc}$** vs. **8H$_{pa}$**	0.20	1.94			
C_{2h} or C_{2h}-like	**8H$_{tt}$** vs. **8H$_{pa}$**	0.06	1.82			
C_i or C_i-like	**8H$_{apa}$** vs. **8H$_{pa}$**	0.00	0.00			
	8H$_{pats}$ vs. **8H$_{pa}$**, A_{rot}	0.03	0.70			
	Acetophenone Azines					
	APFD/6-311G*					
				1M, C_{2h} vs. C_2, A_{en}	0.93	2.15
				2M, C_{2h} vs. C_2, A_{en}	0.96	2.10
Azine twisted	**8M$_{cc}$** vs. **8M$_{tt}$**	0.17	2.42			
C_2 or C_2-like	**8M$_{ct}$** vs. **8M$_{tt}$**, A_{rot}	0.09	0.79			
No azine twist	**8M$_{cc}$** vs. **8M$_{tt}$**	0.18	2.51			
C_{2h} or C_{2h}-like	**8M$_{ct}$** vs. **8M$_{tt}$**, A_{rot}	0.09	0.85	**8M$_{tt}$**, TS vs. M, A_{en}	0.85	1.90
	MP2/6-311G*					
				1M, C_i vs. C_2, A_{en}	1.01	2.03
				1M, C_{2h} vs. C_2	1.30	3.09
				1M, C_{2h} vs. C_i, T_{ph}	0.29	1.06
				2M, C_i vs. C_2, A_{en}	1.03	1.92
				2M, C_{2h} vs. C_2	1.34	2.67
				2M, C_{2h} vs. C_i, T_{ph}	0.31	0.75
Azine twisted	**8M$_{ig}$** vs. **8M$_{mg}$**	0.03	0.32			
C_2 or C_2-like	**8M$_{og}$** vs. **8M$_{mg}$**	−0.03	0.48			
	8M$_{mts}$ vs. **8M$_{mg}$**, A_{rot}	0.05	0.69			
No azine twist	**8M$_{cc}$** vs. **8M$_{pa}$**	0.54	5.02			
C_{2h} or C_{2h}-like	**8M$_{tt}$** vs. **8M$_{pa}$**	0.39	4.86			
	8M$_{ct}$ vs. **8M$_{pa}$**	0.47	4.52			
	8M$_{apa}$ vs. **8M$_{pa}$**	0.02	0.18	**8M$_{apafp}$** vs. **8M$_{pa}$**, T_{ph}	0.33	3.01
	8M$_{pats}$ vs. **8M$_{pa}$**, A_{rot}	0.10	0.97	**8M$_{pa}$** vs. **8M$_{mg}$**, A_{en}	0.98	−0.07[c]

[a]All relative energies in kcal/mol.
[b]Methyl rotation barrier A_{rot}, barrier to enantiomerization A_{en}, and phenyl twist preference energy T_{ph}.
[c]Artifact; see text.

to asymmetric and symmetric motions which involve twisting about the C-Ph and C=N bonds (but not about the N-N bond). Consequently, we searched for a C_i-**1M** structure and located a transition state structure with an extremely soft imaginary mode of **i**2.9 cm^{-1} for rotation around the N-N bond and significant phenyl twists of 19.4° (Figure 3). Because of the extremely low curvature of the azine dihedral angle, it is preferable to talk about an azine transition state *region* rather than a transition state *structure* (hence, "TS" in Table 1). The paths for C_2-**1M** ⇌ C_2-**1M'** enantiomerization will be explored in more detail below (section 3.6).

TABLE 3 | Wavenumbers of imaginary modes of stationary structures[a].

	Azine twist	Ph-Me rot.	Ph-Me rot.	C(N)-Ph twist	C(N)-Ph twist
APFD/6-311G*					
Toluene					
T_{ec}, eclipsed, C_s		29.68			
Benzaldehyde azines					
8H$_{cc}$(H, Me, Me), C_{2h}		45.38	45.35		
8H$_{ct}$(H, Me, Me), C_s		45.82			
Acetophenone azines					
1M(Me, Cl, Cl), C_{2h}	20.11				
2M(Me, Br, Br), C_{2h}	19.92				
8M$_{cc}$(Me, Me, Me), C_2		44.85	44.79		
8M$_{ct}$(Me, Me, Me), C_1		44.66			
8M$_{tt}$(Me, Me, Me), C_{2h}	19.54				
8M$_{cc}$(Me, Me, Me), C_{2h}	19.98	47.12	47.09		
8M$_{ct}$(Me, Me, Me), C_s	19.76	47.02			
MP2(full)/6-311G*					
Toluene					
T_{ec}, eclipsed, C_s		62.94			
Benzaldehyde azines					
8H$_{cc}$(H, Me, Me), C_{2h}		72.33	72.32		
8H$_{tt}$(H, Me, Me), C_{2h}		54.57	54.31		
8H$_{ct}$(H, Me, Me), C_s		72.25	53.91		
8H$_{pats}$(H, Me, Me), C_1		54.43			
Acetophenone azines					
1M(Me, Cl, Cl), C_i	2.91				
1M(Me, Cl, Cl), C_{2h}				34.91	23.63
2M(Me, Br, Br), C_i	1.48				
2M(Me, Br, Br), C_{2h}				35.43	23.63
8M$_{mts}$(Me, Me, Me), C_1		53.58			
8M$_{cc}$(Me, Me, Me), C_{2h}	24.19	74.86	74.68	37.25	
8M$_{tt}$(Me, Me, Me), C_{2h}	23.63	54.35	54.32	36.56	
8M$_{ct}$(Me, Me, Me), C_s	23.85	74.10	54.69	36.97	
8M$_{pats}$(Me, Me, Me), C_1		70.40			
8M$_{apafp}$(Me, Me, Me), C_i				36.64	23.68

[a]Absolute values in cm^{-1}.

All the topological features observed for the APFD and MP2 PESs of **1M** also occur for 4-bromoacetophenone azine **2M**. The activation energies for enantiomerization (A_{en} values in Table 2) of the haloacetophenone azines are just about 2 kcal/mol. The APFD free enthalpies result in barriers A_{en} of $\Delta G(\mathbf{1M}) = 2.15$ kcal/mol and $\Delta G(\mathbf{2M}) = 2.10$ kcal/mol, respectively, and the MP2 data give $\Delta G(\mathbf{1M}) = 2.03$ kcal/mol and $\Delta G(\mathbf{2M}) = 1.92$ kcal/mol, respectively.

The energetic benefit associated with the twisting of the phenyls out of the azine plane is quantified by the relative energies of the C_{2h}- and C_i-structures, that is, the T_{ph} values in Table 2. While the

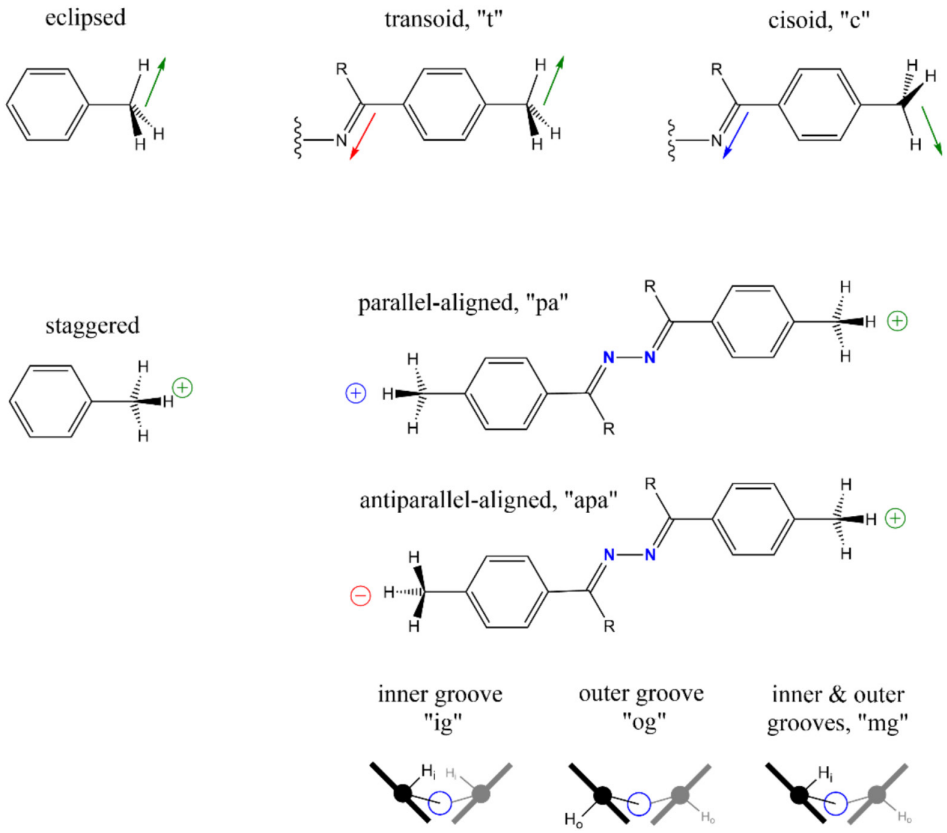

SCHEME 2 | Options and nomenclature for Ph-Me conformations.

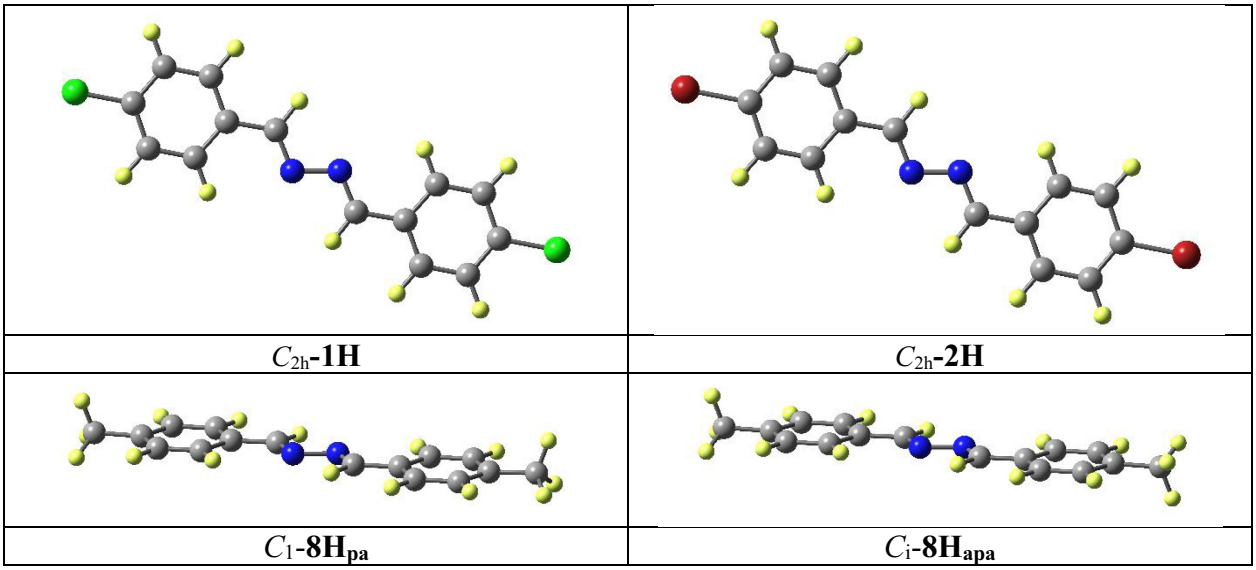

FIGURE 2 | Molecular models of selected structures of benzaldehyde azines optimized at the MP2(full)/6-311G* level.

APFD computations suggest $T_{ph}=0$, the MP2 data for the haloacetophenone azines show small but significant T_{ph} values of $\Delta E(\mathbf{1M})=0.29$ kcal/mol and $\Delta E(\mathbf{2M})=0.31$ kcal/mol, respectively.

3.5 | Para-Methylacetophenone Azine

As with para-tolualdehyde azine **8H**, eclipsed Ph-Me conformations in **8M** are preferred at the APFD/6-311G* level. Three stationary structures with azine twists were located. C_2-**8M$_{tt}$** is the minimum, and C_2-**8M$_{cc}$** is a SOSP (**i**44.85 cm^{-1}, **i**44.79 cm^{-1}, methyl rotations). We also optimized a C_1-**8M$_{ct}$** stationary structure with an overall C_2-like shape but one cisoid and one transoid Me-Ph eclipsed conformation to a first-order saddle point (**i**44.66 cm^{-1}, methyl rotation). The relative energy of C_1-**8M$_{ct}$** compared to C_2-**8M$_{tt}$** specifies the barrier for methyl rotation about the Me-Ph bond A_{rot}, and we find $\Delta G(\mathbf{8M})=0.79$ kcal/mol.

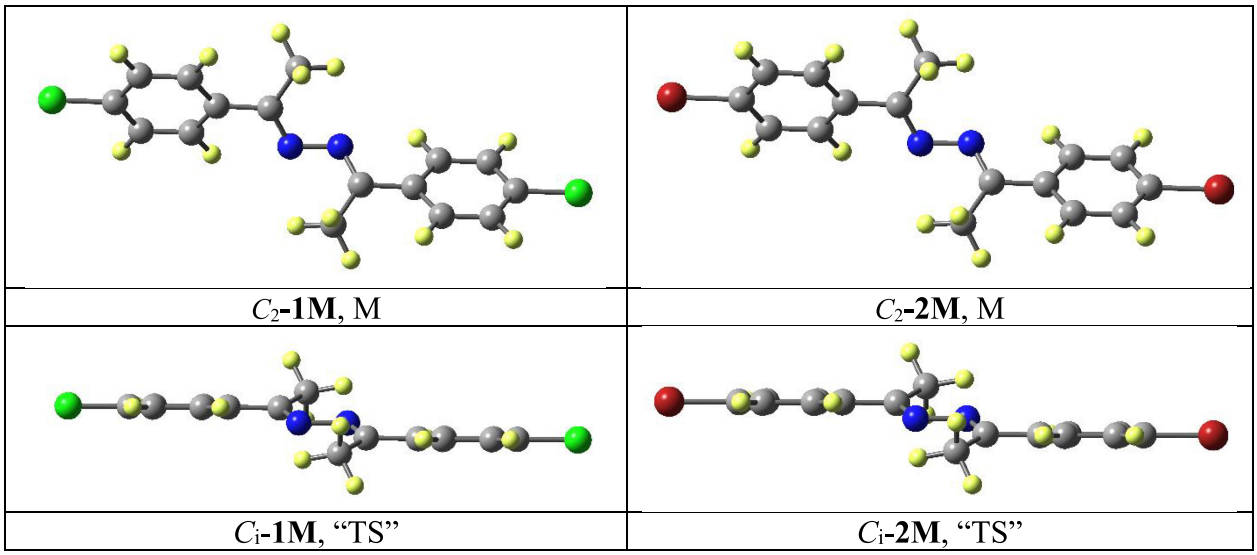

FIGURE 3 | Molecular models of selected structures of para-haloacetophenone azines optimized at the MP2(full)/6-311G* level.

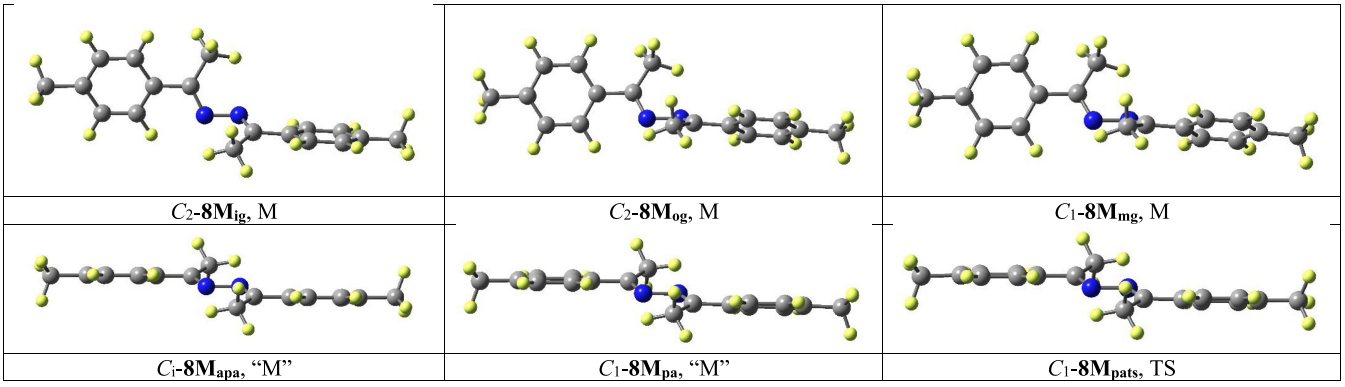

FIGURE 4 | Molecular models of selected structures of para-methylacetophenone azines optimized at the MP2(full)/6-311G* level. Top row: Left arene in the plane. Azine twist and disrotatory phenyl twists cause arenes to be in near-orthogonal planes. Bottom row: Conrotatory phenyl twists cause arenes to be in parallel or near-parallel planes.

We also searched the APFD PES for similar stationary structures *without* azine twist and located structures C_{2h}-**8M**$_{tt}$ (TS), C_{2h}-**8M**$_{cc}$ (TOSP), and C_s-**8M**$_{ct}$ (SOSP). These structures are the analogs to C_2-**8M**$_{tt}$ (M), C_2-**8M**$_{cc}$ (SOSP), and C_1-**8M**$_{ct}$ (TS), but each contains one more imaginary mode for the azine twist angle of about **i**20 cm^{-1} (Table 3). Structure C_{2h}-**8M**$_{tt}$ serves as the transition state structure for enantiomerization C_2-**8M**$_{tt}$ ⇌ C_2-**8M**$_{tt}$'. Hence, we can determine the activation energy for enantiomerization A_{en} of acetophenone azine **8M** as the relative energy of C_{2h}-**8M**$_{tt}$ compared to C_2-**8M**$_{tt}$, and the resulting value $\Delta G = 1.90$ kcal/mol for A_{en}(**8M**) is just slightly lower than for the haloacetophenone azines **1M** and **2M** (Table 3). The energies of C_s-**8M**$_{ct}$ and C_{2h}-**8M**$_{tt}$ allow for another estimate of the barrier for methyl rotation about the Me-Ph bond A_{rot} and result in the value ΔG(**8M**) = 0.85 kcal/mol, very similar to the barrier determined for the C_2-shaped molecules.

The analysis of the MP2/6-311G* PES of **8M** revealed two theoretical level dependencies. The first is familiar from the discussion of **8H**, namely, the preference at the MP2 level for staggered Me-Ph bond conformations in agreement with toluene. The second theoretical level dependency concerns the occurrence of local minima without azine twist.

We located three minima for azine-twisted **8M,** and they are C_2-**8M**$_{ig}$, C_2-**8M**$_{og}$, and C_1-**8M**$_{mg}$ with a small preference for the latter (Table 2 and Figure 4). We also searched for a transition state structure C_1-**8M**$_{mts}$ for methyl rotation (**i**53.58 cm^{-1}) in C_1-**8M**$_{mg}$ to obtain an estimate of ΔG(**8M**) = 0.69 kcal/mol for the barrier to methyl rotation A_{rot}.

An interesting theoretical level dependency relates to the nature of the stationary structures of **8M** *without* azine twist. While no such structure corresponded to a local minimum on the APFD surface, the stationary structures C_i-**8M**$_{apa}$ and C_1-**8M**$_{pa}$ are formally local minima, that is, all vibrational frequencies are real. The vibrational mode associated with τ deformation in the region around $\tau \approx 180°$ is very soft (< 5 cm^{-1} for **8M**$_{apa}$ and **8M**$_{pa}$), and neither of these minima is bound and hence "M" in Table 1. Both structures feature staggered Me-Ph conformations with the unique methyl C → H bond vectors either antiparallel aligned ("apa") or parallel aligned ("pa"), respectively, and both structures feature phenyl twists.

We located the transition state structure for methyl rotation C_1-**8M**$_{\mathbf{pats}}$ which has one staggered and one eclipsed Me-Ph conformation and determined the barrier for methyl rotation A_{rot} to be $\Delta G = 0.97$ kcal/mol. For completeness, we also located C_{2h}-**8M**$_{\mathbf{cs}}$, C_{2h}-**8M**$_{\mathbf{tt}}$, and C_s-**8M**$_{\mathbf{ct}}$ with their eclipsed Ph-Me conformations, and they are the fourth-order saddle points (Table 3).

To estimate the energetic benefit T_{ph} associated with phenyl twisting around the C(N)-Ph bonds, we optimized the C_i-**8M**$_{\mathbf{apafp}}$ structure with constraints $\tau = 180°$ and $\phi_1 = \phi_2 = 0°$. The resulting SOSP structure features two imaginary modes associated with conrotatory and disrotatory rotations about the (N)C-Ph bonds. The relative energy of C_i-**8M**$_{\mathbf{apafp}}$ compared to C_1-**8M**$_{\mathbf{pa}}$ results in an estimate of the phenyl twist preference energy T_{ph} of $\Delta E(\mathbf{8M}) = 0.33$ kcal/mol, a value that is very similar to the T_{ph} values $\Delta E(\mathbf{1M}) = 0.29$ kcal/mol and $\Delta E(\mathbf{2M}) = 0.31$ kcal/mol.

The activation free enthalpies for enantiomerization computed for the haloacetophenone azines are just about 2 kcal/mol (vide supra). Similarly, an enantiomerization energy A_{en} of $\Delta G(\mathbf{8M}) = 1.90$ kcal/mol results at the APFD level (Table 2). The situation is slightly more involved at that MP2 level because the best structure without an azine twist **8M**$_{\mathbf{pa}}$ also is a shallow minimum (as opposed to being a transition state structure). Computing A_{en} using the most stable structures with and without azine-twist and with the MP2 total energies, one obtains $\Delta E(\mathbf{8M}) = 0.98$ kcal/mol, a value that is in line with the other systems. However, based on the free enthalpies one would formally obtain an A_{en} value of $\Delta G(\mathbf{8M}) = -0.07$ kcal/mol. If the structure without azine twist is a shallow TS structure, then the τ deformation mode is the transition vector and the mode does not contribute to thermal energy and molecular entropy. If the structure without azine twist formally becomes a "very shallow minimum", then the τ deformation mode formally contributes to thermal energy and molecular entropy and therefore artificially stabilizes the structure on the ΔG surface. This is clearly an artifact because the "very shallow minimum" is not bound, that is, a τ deformation mode of azine-twisted **8M**$_{\mathbf{mg}}$ would bring the structure into the trans azine region of **8M**$_{\mathbf{pa}}$ and continue to deform the structure into enantiomer **8M**$_{\mathbf{mg}}$'.

3.6 | C_i-Type Plateau Transition Regions and Enantiomerization Paths

3.6.1 | C_i-Type Transition Plateau Region

At the DFT level, the structures C_{2h}-**1M** (**i**20.1 cm^{-1}), C_{2h}-**2M** (**i**19.9 cm^{-1}), and C_{2h}-**8M**$_{\mathbf{tt}}$ (**i**19.5 cm^{-1}) are transition state structures for rotation around the azine bond. Hence, the DFT results would imply that both Ph twists and the azine twist invert at the same time. In contrast, the structures C_{2h}-**1M** (**i**34.9 cm^{-1}, **i**23.6 cm^{-1}) and C_{2h}-**2M** (**i**35.4 cm^{-1} and **i**23.6 cm^{-1}) correspond to SOSPs at the MP2 level. The displacement vectors of the imaginary modes correspond to Ph twisting while maintaining either C_i- or C_2-symmetry, respectively. The C_2-distortion connects these structures to their most stable and azine-twisted C_2-minima. The C_i-distortions lead to the trans-azine structures C_i-**1M**, C_i-**2M** and conformers C_i-**8M**$_{\mathbf{apa}}$ and C_1-**8M**$_{\mathbf{pa}}$ (Figures 3 and 4), and these structures feature pronounced phenyl twists which provide energetic benefits of about 0.3 kcal/mol (T_{ph} values in Table 2).

The conformational space in the region around the C_i-structures is relevant to acetophenone azine enantiomerization and warranted further exploration with the results displayed in Figure 5. While C_i-**1M** and C_i-**2M** *formally* are transition state structures with very small imaginary modes (**i**2.9 cm^{-1} and **i**1.5 cm^{-1}) associated with their azine twists, the structures C_i-**8M**$_{\mathbf{apa}}$ and C_1-**8M**$_{\mathbf{pa}}$ *formally* are minima with very small but real azine twisting modes (4.4 and 3.1 cm^{-1}). These apparent differences obscure the most important PES characteristic common to all azines, namely, the occurrence of *extended transition plateau regions containing C_i-type structures*.

We scanned the MP2(full)/6-311G* PES in the vicinity of the C_i-structures. Using C_i-**1M**, C_i-**2M**, and C_i-**8M**$_{\mathbf{apa}}$ as initial trial structures, we scanned the PESs as a function of the azine angle (Figure 5, left column) and found that the conrotatory Ph twists are retained for some 11°–14° in an essentially isoenergetic region (curve shown with red circle marks). Beyond that region, one of the Ph groups had rotated so that the structures with disrotatory Ph twisting occurred (curve shown with blue triangle marks corresponds to C_2-like Ph twists). Clearly, the C_i-structures are neither TS structures in the classical sense (i.e., with steep declines toward two associated minima) nor are they bound minima. Instead, the C_i-**1M** and C_i-**2M** structures with $\tau = 180°$ are merely at the center of a plateau region of the PES with C_i-type structures in the extended $170° < \tau < 190°$ region. Similarly, the structures C_i-**8M**$_{\mathbf{apa}}$ and C_1-**8M**$_{\mathbf{pa}}$ merely happen to be in the centers of regions containing huge ensembles of (near)trans-azine structures.

3.6.2 | Enantiomerization Between $C_2(M)$ and $C_2'(P)$

The enantiomerization C_2-**1M** $\rightleftharpoons$ C_2-**1M'** requires the azine twist to increase from $\tau = 126.7°$ to 180° and on to $\tau = 233.3°$ ($= -126.7°$) and twisting about both (N)C-Ph bonds. To explore the (τ, ϕ_1) 2D-region of the PES, we performed scans to connect a C_i-type structure (phenyl twists with opposite signs) to a C_2-type structure (phenyl twists both positive or both negative) for fixed azine dihedral angles τ. For the *M* stereoisomer, both Ph twists are positive with $\tau = -126.7°$ or equivalently $\tau = +233.3°$. We show the positive τ values in the left column of Figure 5, and we keep with those values in the plots shown in the right column of Figure 5.

The (τ, ϕ_1) plots are very much the same for **1M**, **2M**, and **8M**, and we discuss **1M**. The four scans shown in Figure 5 (top right) are for structures of **1M** with τ values of 180° (solid squares in purple), 191.5° (or −168.5°, solid square marks in dark green), 200° (or −160°, solid circles in yellow), and 233.3° (or −126.7°, solid circles in blue), and each scan shows the result of the rotation of the phenyl group with the negative twist in the C_i-structure. For $\tau = 233.3°$, this Ph rotation leads to enantiomer $C_2(M)$ of **1M**. Had we scanned the rotation of the phenyl group with the positive twist, we would have ended up with profiles that are symmetric about the vertical line at $\phi = 0$ and reaching

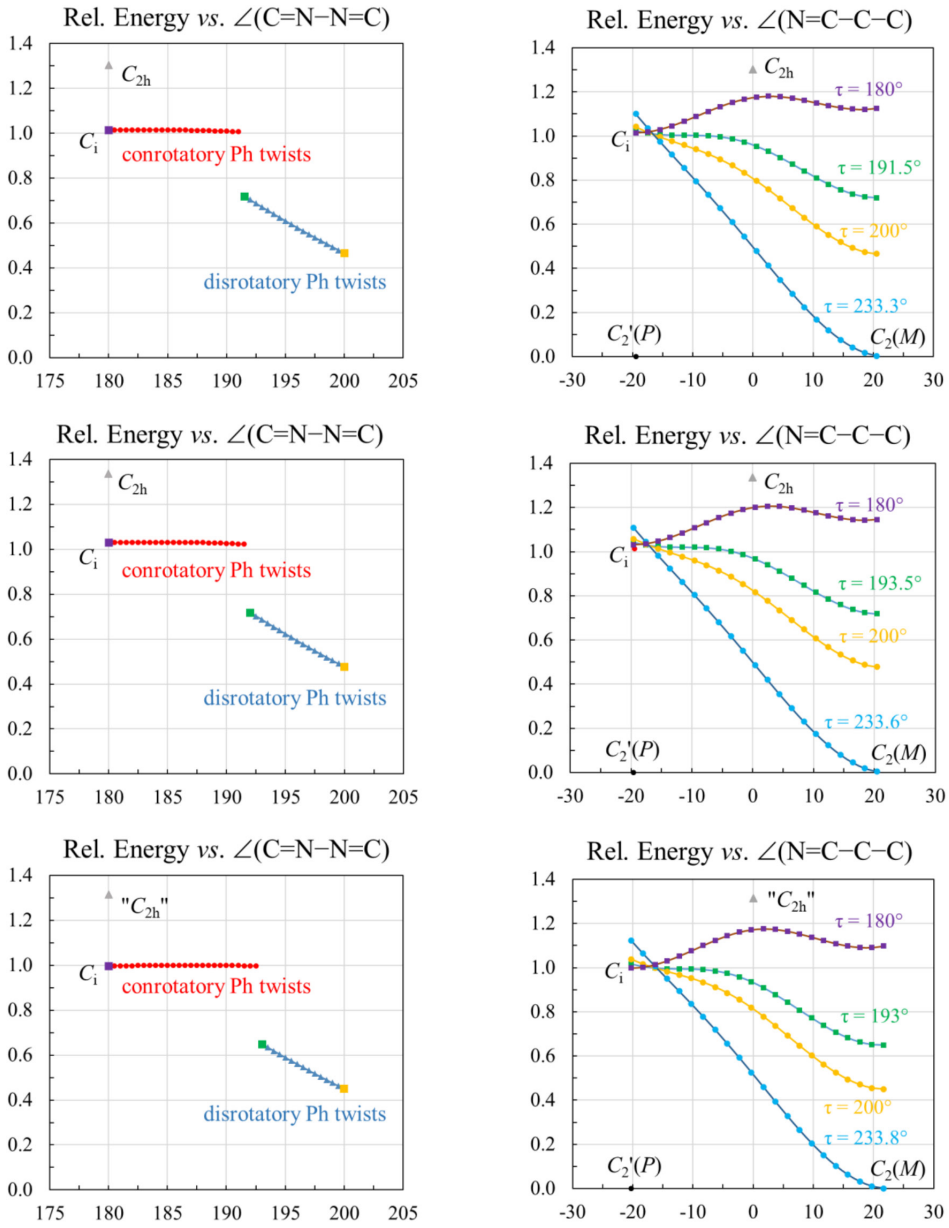

FIGURE 5 | Exploration of the enantiomerization paths. MP2(full)/6-311G* energies relative to C_2-**1M** (top), **2M** (center), and **8M** (bottom) in kcal/mol are shown as a function of the azine dihedral angle τ (left) and as a function of the Ph dihedral angle ϕ with fixed azine twists (right).

enantiomer C_2'(*P*). Note that C_{2h}-**1M** with $\phi_1 = \phi_2 = 0°$ is less stable than the maximum of the $\tau = 180°$ scan. With the azine twist set to $\tau = 180°$, a very small barrier to (N)C-Ph rotation occurs. As ϕ_1 increases, however, there will be a more stable structure with a larger azine twist τ, and the resulting intrinsic reaction path in (τ, ϕ_1) space will be downhill all the way.

The (τ, ϕ) 2D scans reveal that the C_i-symmetric plateau region of the PES spans a larger (τ, ϕ_1, ϕ_2) space. Most importantly, the results of the PES explorations show that the enantiomerization (*M*)-enantiomer ⇌ (*P*)-enantiomer of C_2-type azines involves three steps: (i) a first (N)C-Ph rotation to convert a C_2-like structure (disrotatory phenyl twists) to a C_i-like structure (conrotatory phenyl twists), (ii) rotation about the N-N bond through the azine twist angle $\tau = 180°$ in the C_i-type transition plateau region, and (iii) a second (N)C-Ph rotation to convert the C_i-type structure to the enantiomeric C_2-type structure.

In the context of the analyses of polymorph **II** crystal structures, the PES analyses allow for two important conclusions. While C_{2h}-symmetric structures are the only minima for the benzaldehyde azines, the *only* minima of free acetophenone azines are C_2-type structures with twisted azines. For emphasis, we state the corollary; that is, there are no bound C_i-type local minima on the PESs of free acetophenone azines.

3.7 | Steric Strain Associated With Presence of Methyl Groups at Azine-Carbons

The discussion of the theoretical level dependencies showed a clear and consistent difference regarding the Ph-Me conformation. Otherwise, both levels suggest similar conformational and angular trends. Table 4 lists six groups: benzaldehyde azines (Region 1), acetophenone azines with azine twist (Region 2), and

TABLE 4 | Major angles and dihedral angles of pertinent structures computed at APFD/6-311G* and MP2(full)/6-311G*.

Structure	Azine twist τ	Phenyl twist ϕ1	Phenyl twist ϕ2	∠(NNC)	∠(NCR)	∠(NCCPh)	DPA
Benzaldehyde azines, APFD							
C_{2h}-**1H**	180.0	0.0	0.0	112.4	119.8	122.0	9.6
C_{2h}-**2H**	180.0	0.0	0.0	112.4	119.8	122.0	9.6
C_{2h}-**8H$_{tt}$**	180.0	0.0	0.0	112.5	119.6	122.2	9.8
Average	180.0	0.0	0.0	112.4	119.7	122.1	9.6
Std. dev.	0.0	0.0	0.0	0.0	0.1	0.1	0.1
Benzaldehyde azines, MP2							
C_{2h}-**1H**	180.0	0.0	0.0	111.3	119.8	121.4	10.1
C_{2h}-**2H**	180.0	0.0	0.0	111.3	119.8	121.4	10.1
C_i-**8H$_{apa}$**	180.0	0.2	−0.2	111.3	119.7	121.6	10.3
C_1-**8H$_{pa}$**	180.0	−0.2	−0.2	111.3	119.7	121.6	10.3
Average	180.0	0.0	−0.1	111.3	119.7	121.5	10.2
Std. dev.	0.0	0.1	0.1	0.0	0.1	0.1	0.1
Acetophenone azines, APFD							
With azine twist (Region 2)							
C_2-**1M**	132.3	−15.7	−15.7	117.9	123.5	116.8	−1.1
C_2-**2M**	133.0	−15.7	−15.7	117.9	123.5	116.8	−1.2
C_2-**8M$_{tsd}$**	133.7	−15.4	−15.4	117.7	123.3	117.0	−0.7
Average	133.0	−15.6	−15.6	117.9	123.4	116.9	−1.0
Std. Dev.	0.6	0.1	0.1	0.1	0.1	0.1	0.2
Without azine twist (Region 3)							
C_{2h}-**1M** (TS)	180.0	0.0	0.0	115.4	124.9	116.4	0.9
C_{2h}-**2M** (TS)	180.0	0.0	0.0	115.4	124.9	116.3	0.9
C_{2h}-**8M$_{tt}$** (TS)	180.0	0.0	0.0	115.5	124.69	116.6	1.1
Average	180.0	0.0	0.0	115.4	124.8	116.4	1.0
Std. dev.	0.0	0.0	0.0	0.0	0.1	0.1	0.1
Acetophenone azines, MP2							
With azine twist (Region 2)							
C_2-**1M**	126.7	−21.9	−21.9	115.8	123.6	116.2	0.4
C_2-**2M**	126.5	−22.0	−22.0	115.8	123.6	116.2	0.4
C_2-**8M$_{ig}$**	126.3	−22.7	−22.7	115.7	123.4	116.4	0.7
C_2-**8M$_{og}$**	126.0	−22.4	−22.4	115.7	123.4	116.4	0.7
C_2-**8M$_{mg}$**	126.2	−22.7	−22.4	115.8	123.4	116.4	0.7
Average	126.3	−22.3	−22.3	115.8	123.5	116.3	0.6
Std. dev.	0.2	0.3	0.3	0.0	0.1	0.1	0.1
Without azine twist (Region 3)							
C_i-**1M** ("TS")	180.0	−19.4	19.4	113.8	125.4	115.6	1.9
C_i-**2M** ("TS")	180.0	−19.7	19.7	113.8	125.4	115.6	1.8

(Continues)

TABLE 4 | (Continued)

Structure	Azine twist τ	Phenyl twist ϕ1	Phenyl twist ϕ2	∠(NNC)	∠(NCR)	∠(NCCPh)	DPA
C_i-**8M**$_{apa}$	180.0	−20.3	20.3	113.8	125.3	115.8	2.0
C_1-**8M**$_{pa}$	176.1	−20.8	19.2	113.9	125.2	115.8	2.0
Average	179.0	−20.1	19.6	113.8	125.3	115.7	1.9
Std. dev.	1.7	0.5	0.4	0.0	0.1	0.1	0.1

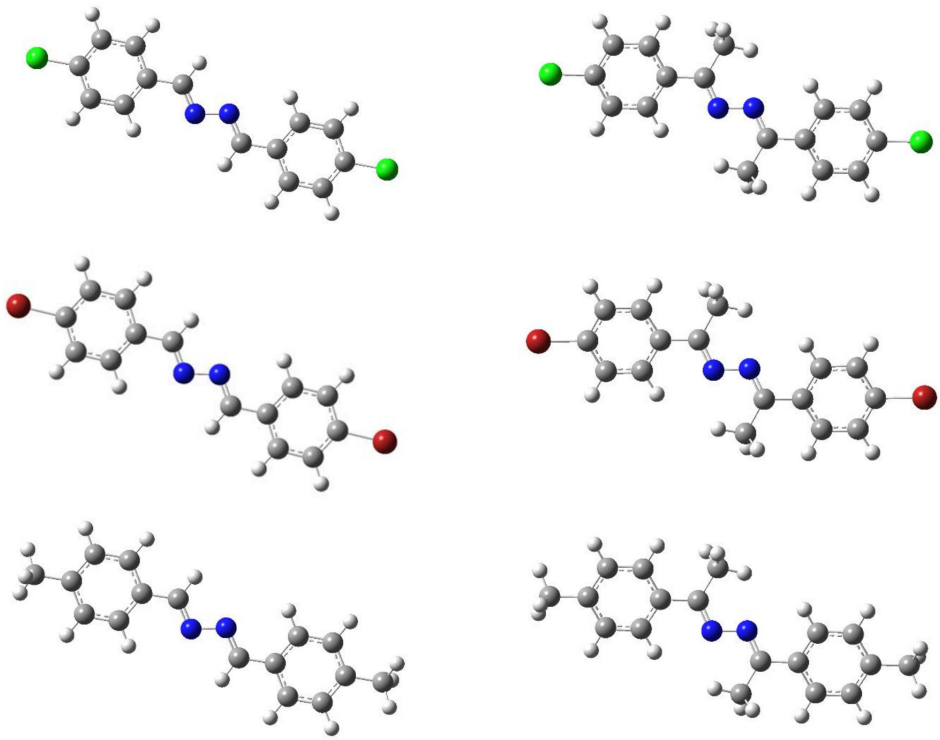

FIGURE 6 | Comparison of the MP2(full)/6-311G* optimized minima of benzaldehyde azine C_{2h}-**1H**, C_{2h}-**2H**, and C_i-**8H**$_{apa}$ (left column) and the C_i-symmetric stationary acetophenone azine structures C_i-**1M**, C_i-**2M**, and C_i-**8M**$_{apa}$ (right column).

acetophenone azines without azine twist (Region 3), respectively, at levels APFD and MP2, respectively. For each group, averages and standard deviations are provided. The standard deviations are very small and thus fully warrant the discussion of groups.

The benzaldehyde azines show trans-azine frames without phenyl twists, and there is hardly any difference between the APFD and MP2 results. There also is nothing unusual about the angles at the azine carbons; the angles ∠(N-C-H) and ∠(N-C-C_{Ph}) are close to sp^2-hybridization angles. The only remarkable angular feature concerns the angles ∠(N-N-C) at the azine N-atoms; they are 112° ± 1°. This angular depression may serve to place the azine-Hs closer to proximate N's lone pair. The angular depression at the N-atoms causes a deviation from parallel alignment of the N-N and C-Ph bonds by DPA = ∠(N-C-C_{Ph}) - ∠(N-N-C) ≈ 10° and is well illustrated in Figure 6.

The acetophenone azines prefer twisted azine frames with phenyl twists with APFD data ($\tau = 133.0 \pm 0.6°$, $|\phi| = 15.6 \pm 0.1°$) suggesting more azine twist and less phenyl twist compared to the MP2 results ($\tau = 126.3 \pm 0.3°$, $|\phi| = 22.3 \pm 0.3°$). In contrast to the benzaldehyde azines, the acetophenone azines without azine twists do feature phenyl twists, and the phenyl twists again are significantly less at the APFD level ($|\phi| = 15.6 \pm 0.1°$) compared to the MP2 level ($|\phi| = 20 \pm 1°$).

The methyl groups attached to the azine C-atoms assume the Az-Me conformation that places one methyl-H close to a proximate azine N-atom with the other two methyl-Hs staggering the ortho CH hydrogen. The ∠(N-N-C) angles increase by about 3°–6°; they all remain well below 120° indicative of the engagement of the azine methyl groups in intramolecular C-H···N hydrogen bonding. The steric demand of the methyl groups gives ∠(N-C-C_{Me}) angles that are about 3°–5° larger and ∠(N-C-C_{Ph}) angles that are about 6°–7° smaller compared to the benzaldehyde azines. The DPA values of the acetophenone azines are less than 2° (Table 4).

3.8 | Phenyl Twists in Acetophenone Azines: Azine-Methyls Make All the Difference

What causes the phenyl twisting in the $\tau \approx 180°$ region of acetophenone azines **1M**, **2M**, and **8M** when the benzaldehyde

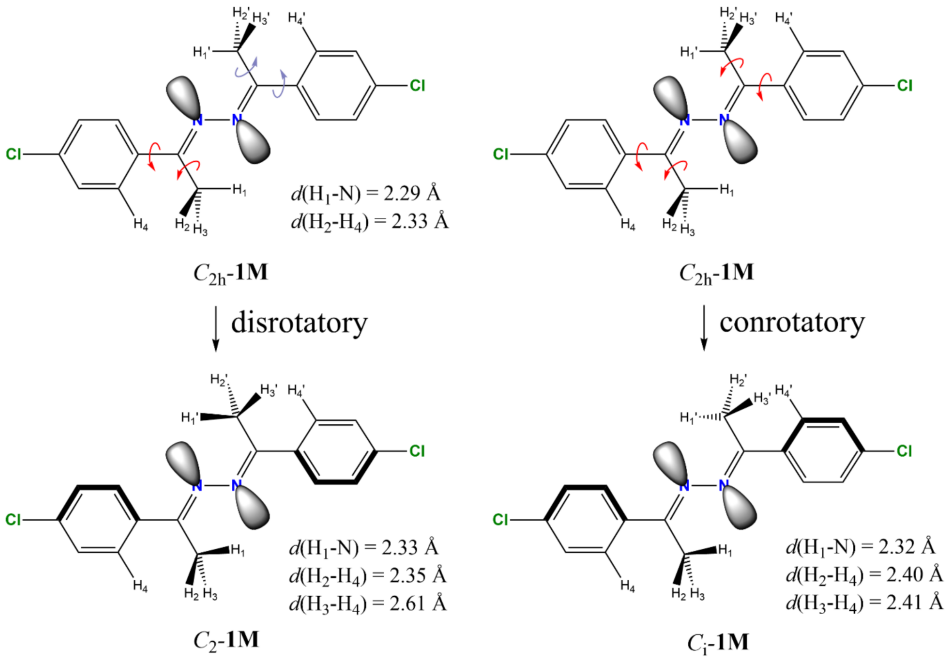

SCHEME 3 | Steric interaction between nitrogen lone pairs and azine methyl hydrogens causes methyl rotations and correlated phenyl twists.

azine **1H**, **2H**, and **8H** are perfectly happy being planar? Figure 6 provides a hint, and Scheme 3 helps to explain using **1M** as example.

In Figure 6, we aligned the N-N bonds of C_{2h}-**1H** and C_i-**1M** to be parallel. It is immediately obvious that the ∠(N-C-R) angle is much larger in the presence of the methyl group (125.4°, R = Me) than in its absence (119.8°, R = H). Most of this angular change is compensated by the smaller ∠(N-C-C_{Ph}) angle in **1M** (115.6°) compared to **1H** (121.4°). In azine **1H**, the azine-H does not pose any serious steric strain. In C_{2h}-**1H**, the nonbonded distance $d(H\cdots H_{ortho}) = 2.43$ Å is larger than the (H,H) van der Waals contact distance of 2.40 Å [47], while the nonbonded distance $d(H\cdots N) = 2.37$ Å is well within the (H,N) v.d.W. contact of 2.75 Å. The steric situation changes drastically in the acetophenone azine **1M**. One methyl-H_1 in C_{2h}-**1M** points toward an azine-N so that the H_2 and H_3 atoms are staggered with the proximate *ortho*-H. This conformation places H_1 well within v.d.W. distance of the azine-N and $d(H_1\cdots N) = 2.29$ Å, and importantly, the Az-Me group causes steric interference with the *ortho*-H as evidenced by the v.d.W. distances in Scheme 3.

There are two ways to avoid the close H···N contacts while maintaining C-H···N hydrogen bonding, and these are illustrated in Scheme 3. Considering the left half of the molecule first, the rotation of the methyl group that moves H_1 above the paper plane will reduce the (H,N)-strain. As a direct consequence of this methyl group rotation, the phenyl group must rotate to maintain the staggered arrangement of *ortho*-H_4 with methyl hydrogens H_2 and H_3. Such a geared rotation [48, 49] of the methyl and phenyl groups also must happen in the other half of the molecule—and there are two options. On the left side of Scheme 3, the second methyl group is rotated in a way that H_4' is placed above the paper plane (and on the same face as H_4). The geared rotation thus leads to disrotatory Ph twists and C_2 symmetry. And the right side of Scheme 3 shows the outcome resulting from the rotation of the second methyl group in the opposite direction: conrotatory Ph twists and C_i-symmetry.

4 | Conclusion

At the MP2(full)/6-311G* level benzaldehyde azines, **1H**, **2H**, and **8H** are trans-azines ($\tau = 180°$) without phenyl twist (C_{2h}-**1H**, C_{2h}-**2H**) or with only tiny phenyl twists (C_i-$\mathbf{8H_{apa}}$, C_1-$\mathbf{8H_{ap}}$). At the same MP2 level, the C_2-symmetric minima of acetophenone azines **1M**, **2M**, $\mathbf{8M_{ig}}$, and $\mathbf{8M_{og}}$ feature twisted azines spacers ($\tau \approx 126°$) and disrotatory phenyl twists ($\phi_i \approx -22°$). Structures of the acetophenone azines with trans-azine spacers ($\tau = 180°$) exhibit conrotatory phenyl twists ($|\phi_i| \approx 20°$) and are C_i-symmetric (**1M**, **2M**, and $\mathbf{8M_{apa}}$) or of similar shape (C_1-$\mathbf{8M_{pa}}$). 2D-scans of the PESs of acetophenone azines **1M**, **2M**, and **8M** in the regions of transoid acetophenone azines (τ region of 180° ± 10°) all demonstrate essentially flat plateaus as their common feature: The structures C_i-**1M** and C_i-**2M** formally are transition state structures but with exceedingly low imaginary modes, and C_i-$\mathbf{8M_{apa}}$ and C_1-$\mathbf{8M_{pa}}$ are merely very shallow unbound minima. Hence, our analyses show that the *only* minima of free acetophenone azines are C_2-type structures with twisted azines; that is, there are no bound C_i-type local minima on the PESs of free acetophenone azines.

A few differences have been noted between the MP2 and APFD studies. To begin with, the toluyl-methyl groups prefer eclipsed conformation at the APFD level while staggered conformations are consistently preferred at the MP2 level and at higher MPx//MP2 levels. This is a minor issue because rotations about the Ph-Me bonds are essentially free. A more significant theoretical level dependency concerns the phenyl twisting in the acetophenone azines. While MP2 structures show disrotatory or conrotatory phenyl twists on the order of 20° for C_2-type and C_i-type structures, respectively, the APFD results suggest smaller

disrotatory phenyl twists on the order of only 15° for the C_2-type structures and, notably, no phenyl twist at all for the C_i-type azines. This is a systematic difference that reflects on the methods' abilities to properly handle intramolecular through-space interactions, which are dominated by van der Waals binding. While the through-space 1,4-contact between a polar C-H bond hydrogen and the proximate azine-N is *attractive* in benzaldehyde azines, the azine-Me groups in acetophenone azines cause steric *repulsion* with the N lone pairs: two 1,5-contacts between nonpolar methyl C-H bond hydrogens and the close-by azine-N lone pairs. This strain can be reduced with adequate accounting for dynamic electron correlation at the MP2 level, and adopting structures with small rotations about the Az-CH_3 bonds and geared phenyl twisting may lead to C_2- or C_i-structures.

The exploration of the (τ, ϕ_1, ϕ_2) space on the MP2(full)/6-311G* PES of **1M** shows that the enantiomerization of C_2-**1M** to C_2-**1M'** occurs in the extended plateau region containing transoid azine structure and involves first one Ph twist inversion to a C_i-like structure, then the inversion of the azine twist in the C_i-symmetric plateau region, followed by the second Ph twist inversion on the path to C_2-**1M'**. The essential characteristics of this enantiomerization mechanism apply in general to disubstituted acetophenone azine, and the process is facile. The conformation of azines is fluxional with only small barriers to phenyl twisting ($T_{ph} < 0.3$ kcal/mol) and enantiomerization ($A_{en} < 1.5$ kcal/mol), and it is this conformational flexibility that allows for the creation of a rich variety of supramolecular architectures in 1,4-diphenylazine crystals.

Author Contributions

Rainer Glaser: writing – original draft, writing – review and editing, project administration, funding acquisition, formal analysis, conceptualization, methodology, visualization, validation. **Kaidi Yang:** Writing – original draft, Writing – data acquisition, formal analysis, methodology, visualization, validation. **Harmeet Bhoday:** Writing – review and editing, Writing – formal analysis, visualization, validation.

Acknowledgments

This work was supported by the Missouri University of Science and Technology and, in part, by a grant from the National Science Foundation #1665487. We gratefully acknowledge generous access to the MILL cluster (https://doi.org/10.71674/PH64-N397).

Conflicts of Interest

The authors declare no conflicts of interest.

Data Availability Statement

The data that support the findings of this study are openly available in the Supporting Information.

References

1. J. Safari and S. Gandomi-Ravandi, "Structure, Synthesis and Application of Azines: A Historical Perspective," *RSC Advances* 4 (2014): 46224–46242.

2. S. S. Chourasiya, D. Kathuria, and A. A. Wani, "Azines: Synthesis, Structure, Electronic Structure and Their Applications," *Organic & Biomolecular Chemistry* 17 (2019): 5498–5516.

3. L. Jin, Y. Xie, C. Lin, S. Han, D. Shi, and H. Yu, "A Simple and Efficient Method for the Nickel-Catalyzed Synthesis of Azines From Aldehydes and Hydrazines," *ChemistrySelect* 9 (2024): e202304446 (6 p.).

4. Y. Wang, Z.-Z. Guo, J.-P. Qu, and Y.-B. Kang, "Photocatalytic One-Step Synthesis of Unsymmetrical Azines," *Organic Letters* 27 (2025): 1626–1630.

5. A. Alam, F. U. Rahman, A. A. Elhenawy, and A. Ali, "Exploring the Versatility of Azine Derivatives: A Comprehensive Review on Synthesis and Biological Applications," *Mini-Reviews in Medicinal Chemistry* 25 (2025): 425–439.

6. G. Kim, J. Yang, and N. Nakashima, "Highly Microporous Nitrogen-Doped Carbon Synthesized From Azine-Linked Covalent Organic Framework and Its Supercapacitor Function," *Chemistry-A European Journal* 23 (2017): 11423–11429.

7. S. Poojary, D. Sunil, D. Kekuda, and S. Sreenivasa, "Fluorescent Aromatic Symmetrical Azines: Synthesis and Appraisal of Their Photophysical and Electrochemical Properties," *Optical Materials* 86 (2018): 366–373.

8. B. Vercelli, M. Pasini, A. Berlin, et al., "Phenyl- and Thienyl-Ended Symmetric Azomethines and Azines as Model Compounds for n-Channel Organic Field-Effect Transistors: An Electrochemical and Computational Study," *Journal of Physical Chemistry C* 118 (2014): 3984–3993.

9. P. Acker, M. E. Speer, J. S. Wössner, and B. Esser, "Azine-Based Polymers With a Two-Electron Redox Process as Cathode Materials for Organic Batteries," *Journal of Materials Chemistry A* 8 (2020): 11195–11201.

10. W. Hong, C. Guo, B. Sun, and Y. Li, "(3*Z*,3′*Z*)-3,3′-(Hydrazine-1,2-diylidene)bis(indolin-2-one) as a New Electron-Acceptor Building Block for Donor–Acceptor π-Conjugated Polymers for Organic Thin Film Transistors," *Journal of Materials Chemistry C* 3 (2015): 4464–4470.

11. R. Glaser, "Polar Order by Rational Design: Crystal Engineering With Parallel Beloamphiphile Monolayers," *Accounts of Chemical Research* 40 (2007): 9–17, https://doi.org/10.1021/ar0301633.

12. M. Lewis, Z. Wu, and R. Glaser, ""Arene-Arene Double T-Contacts. Lateral Synthons in the Engineering of Highly Anisotropic Organic Crystals," Chapter 7 in "Anisotropic Organic Materials - Approaches to Polar Order"," in *ACS Symposium Series*, vol. 798, eds. R. Glaser and P. Kaszynski (American Chemical Society, 2001), 97–111.

13. M. Lewis and R. Glaser, "The Azine Bridge as a Conjugation Stopper: An NMR Spectroscopic Study of Electron Delocalization in Acetophenone Azines," *Journal of Organic Chemistry* 67 (2002): 1441–1447, https://doi.org/10.1021/jo011117o.

14. M. Lewis, C. Barnes, and R. Glaser, "4-Chloroacetophenone-(4-methoxyphenylethylidene) hydrazone," *Acta Crystallographica. Section C* 56 (2000): 393–396, https://doi.org/10.1107/S0108270199011737 "4-Chloroacetophenone-4-Methoxyacetophenone Azine," *CCDC Communication* (2000): 143276 (CODRES). CCDC.

15. G. S. Chen, J. K. Wilbur, C. L. Barnes, and R. Glaser, "Push-Pull Substitution Versus Intrinsic or Packing Related N-N Gauche Preferences in Azines. Synthesis, Crystal Structures and Packing of Asymmetrical Acetophenone Azines," *Journal of the Chemical Society, Perkin Transactions 2* 12 (1995): 2311–2317, https://doi.org/10.1039/P29950002311 ZIFBUL, 1312232, "4-Bromoacetophenone 4-Methoxyacetophenone Azine.".

16. M. Lewis, C. Barnes, and R. Glaser, "Near-Perfect Dipole Parallel-Alignment in the Highly Anisotropic Crystal Structure of 4-Iodoacetophenone-(4-methoxyphenylethylidene) Hydrazone," *Journal of Chemical Crystallography* 30 (2000): 489–496, https://doi.org/10.1023/A:1011311918880 "4-Methoxyacetophenone-4-Iodoacetophenone Azine," CCDC Communication (2001): 165429 (SUXZAM). CCDC.

17. H. Bhoday, M. Lewis, S. P. Kelley, and R. Glaser, "Perfect Polar Alignment of Parallel Beloamphiphile Monolayers: Synthesis, Characterization, and Crystal Architectures of Unsymmetrical Phenoxy-Substituted Acetophenone Azines," *ChemPlusChem* 87 (2022): e202200224.

18. H. Bhoday, S. Kelley, and R. Glaser, "Polar and Non-Polar Stacking of Perfectly Aligned Parallel Beloamphiphile Monolayers (PBAMs) of

(PhO, F)-Azine. The Interplay of Non-Covalent Interlayer Interactions and Unit Cell Polarity," *CrystEngComm* 25 (2023): 2175–2180.

19. R. Glaser, N. Knotts, P. Yu, et al., "Perfect Polar Stacking of Parallel Beloamphiphile Layers. Synthesis, Structure, and Solid-State Optical Properties of the Unsymmetrical Acetophenone Azine DCA," *Dalton Transactions* 23 (2006): 2891–2899.

20. N. Knotts, R. Glaser, C. Barnes, and S. P. Kelley, "4-Decyloxyacetophenone 4-Fluoroacetophenone Azine," *CCDC Communication* (2020): 2040896 (XUYYEY), https://doi.org/10.5517/ccdc.csd.cc26hqct.

21. N. Knotts, R. Glaser, C. Barnes, and S. P. Kelley, "4-Decyloxyacetophenone 4-Chloroacetophenone Azine," *CCDC Communication* (2020): 2040898 (XUYYOI), https://doi.org/10.5517/ccdc.csd.cc26hqfw.

22. N. Knotts, R. Glaser, C. Barnes, and S. P. Kelley, "4-Decyloxyacetophenone 4-Bromoacetophenone Azine," *CCDC Communication* (2020): 2040895 (XUYYAU), https://doi.org/10.5517/ccdc.csd.cc26hqbs.

23. H. Bhoday, N. Knotts, and R. Glaser, "Perfect Polar Alignment of Parallel Beloamphiphile Layers: Improved Structural Design Bias Realized in Ferroelectric Crystals of the Novel "Methoxyphenyl Series of Acetophenone Azines"," *Chemistry-A European Journal* 30 (2024): e202400182.

24. R. Glaser, G. S. Chen, and C. L. Barnes, "Conjugation in Azines. Stereochemical Analysis of Benzoylformate Azines in the Solid State, in Solution, and in the Gas Phase," *Journal of Organic Chemistry* 58 (1994): 7446–7455, https://doi.org/10.1021/jo00094a059.

25. G. S. Chen, M. Anthamatten, C. L. Barnes, and R. Glaser, "Stereochemistry and Stereoelectronics of Azines. A Solid-State Study of Symmetrical, (*E*,*E*)-Configured, Para-Substituted (H, F, Cl, Br, CN) Acetophenone Azines," *Journal of Organic Chemistry* 59 (1994): 4336–4340, https://doi.org/10.1021/jo00094a059.

26. H. Bhoday, K. Yang, S. Kelley, and R. Glaser, "Crystal Environment Induced Symmetry Reduction (CEISR): Deep Analysis of Para-Chloroacetophenone Azine and Generalization," *CrystEngComm* 25 (2023): 4638–4657.

27. H. Bhoday, K. Yang, S. Kelley, and R. Glaser, "A New Paradigm for the Supramolecular Structure of Laterally Offset Diarenes: Crystal Structures and Stabilities of Polymorphs II of Para-Substituted Acetophenone Azines, Y_p–Ph–(Me)C=N–N=C(Me)–Ph–Y_p (Y = Cl, Br, CH_3)," *European Journal of Organic Chemistry* 28 (2025): e202500713, https://doi.org/10.1002/ejoc.202500713.

28. H. Bhoday, A. Schuman, S. P. Kelley, and R. Glaser, "4-Chloroacetophenone Azine (Polymorph II)," *CCDC Communication* (2020): 2027206 (HUXMEV), https://doi.org/10.5517/ccdc.csd.cc261grh.

29. H. Bhoday, A. Schuman, S. P. Kelley, and R. Glaser, "4-Bromoacetophenone Azine (Polymorph II)," *CCDC Communication* (2023): 2234130 (LIKJEU02), https://doi.org/10.5517/ccdc.csd.cc2dzsqx.

30. G. S. Chen, M. Anthamatten, C. L. Barnes, and R. Glaser, "Polymorphism and Conformational C=N–N=C Bond Isomers of Azines: X-Ray Crystal and Ab Initio Structures of Two Rotameric Structures of Methyl (Para-Tolyl) Ketone Azine," *Angewandte Chemie International Edition in English* 33 (1994): 1081–1083, https://doi.org/10.1002/anie.199410811 CCDC Descriptors: PIYYAX, 1235041, Polymorph A of 2(Me,Me) in Chen et al.; PIYXOK, 1235039, Polymorph B of 2(Me,Me) in Chen et al.

31. J. S. Chen, M. Anthamatten, C. L. Barnes, and R. Glaser, "(*E*,*E*)-P-Chloroacetophenone Azine (100 K)," *CCDC Communication* (1994): 1207287 (LIKHUI).

32. H. Bhoday, A. Schuman, S. P. Kelley, and R. Glaser, "4-Bromoacetophenone Azine (Polymorph I)," *CCDC Communication* (2021): 2056546 (LIKJEU01), https://doi.org/10.5517/ccdc.csd.cc27106j.

33. R. Glaser, R. F. Murphy, Y. Sui, C. L. Barnes, and S. H. Kim, "Multifurcated Halogen Bonding Involving Ph–Cl···H–CPh=N–R' Interactions and Its Relation to Idioteloamphiphile Layer Architecture," *CrystEngComm* 8 (2006): 372–376, https://doi.org/10.1039/b601467d "4-Chlorobenzophenone Azine," CCDC Communication (2006): 292918 (GAVCEM01), CCDC.

34. N. R. L. Correira, T. C. M. Noguiera, A. C. Pinheiro, et al., "Crystal Structures and Hirshfeld Surface Analyses of Halogen Substituted Azine Derivatives, 1,4-Bis(halophenyl)-2,3-diazabuta-1,3-dienes," *Zeitschrift Fuer Kristallographie - Crystalline Materials* 233 (2018): 2017–2081. CCDC Communication (2018): 1551267 (BRBZAL03), CCDC, https://doi.org/10.5517/ccdc.csd.cc1p26wv.

35. R. G. Parr and W. Yang, *Density-Functional Theory of Atoms and Molecules* (Oxford University Press, 1989).

36. A. Austin, G. Petersson, M. J. Frisch, J. Dobek, G. Scalmani, and K. Throssell, "A Density Functional With Spherical Atom Dispersion Terms," *Journal of Chemical Theory and Computation* 8 (2012): 4989–5007.

37. A. D. Mclean and G. S. Chandler, "Contracted Gaussian Basis Sets for Molecular Calculations 1. 2nd Row Atoms, Z = 11-18," *Journal of Chemical Physics* 72 (1980): 5639–5648.

38. K. Raghavachari, J. S. Binkley, R. Seeger, and J. A. Pople, "Self-Consistent Molecular Orbital Methods. XX. Basis Set for Correlated Wave-Functions," *Journal of Chemical Physics* 72 (1980): 650–654.

39. M. J. Frisch, A. Pople, and J. S. Binkley, "Self-Consistent Molecular Orbital Methods 25. Supplementary Functions for Gaussian Basis Sets," *Journal of Chemical Physics* 80 (1984): 3265–3269.

40. C. Møller and M. S. Plesset, "Note on an Approximation Treatment for Many-Electron Systems," *Physical Review* 46 (1934): 618–622.

41. R. F. Fink, "Why Does MP2 Work?," *Journal of Chemical Physics* 145 (2016): 184101–184112.

42. D. Cremer, "Møller–Plesset Perturbation Theory: From Small Molecule Methods to Methods for Thousands of Atoms," *WIREs Computational Molecular Science* 1 (2011): 509–530.

43. M. J. Frisch, G. W. Trucks, and H. B. Schlegel, "Gaussian 16, Revision A.03, Gaussian, Inc., Wallingford CT," (2016).

44. "The Term "Hindered Rotation" Is Used Here to Describe Essentially Free Rotations With Very Small Barriers (Just a Few Calories Per Mole)," This is in contrast to situations where the various conformations are separated by more substantial barriers (a few *kilocalories* per mole) that provide lifetime to each conformation but allow for facile equilibration.

45. R. B. McClurg, R. C. Flagan, and W. A. Goddard, III, "The Hindered Rotor Density-of-States Interpolation Function," *Journal of Chemical Physics* 106 (1997): 6675–6680.

46. P. Y. Ayala and H. N. Schlegel, "Identification and Treatment of Internal Rotation in Normal Mode Vibrational Analysis," *Journal of Chemical Physics* 108 (1998): 2314–2325.

47. A. Bondi, "Van Der Waals Volumes and Radii," *Journal of Physical Chemistry* 68 (1964): 441–451, https://doi.org/10.1021/j100785a001.

48. S. Grilli, L. Lunazzi, A. Mazzanti, D. Casarini, and C. Femoni, "Conformational Studies by Dynamic NMR. 78. Stereomutation of the Helical Enantiomers of Trigonal Carbon Diaryl-Substituted Compounds: Dimesitylketone, Dimesitylthioketone, and Dimesitylethylene," *Journal of Organic Chemistry* 66 (2001): 488–495.

49. T. Tseng, H.-F. Lu, C.-Y. Kao, et al., "Redox-Gated Tristable Molecular Brakes of Geared Rotation," *Journal of Organic Chemistry* 82 (2017): 5354–5366.

Supporting Information

Additional supporting information can be found online in the Supporting Information section. **TABLE S1:** Total energies and thermochemical data of toluene. **TABLE S2:** Higher level MPx energies of toluene. **TABLE S3:** Conformation preference energies of toluene a.